Final Report

EXPERIMENTAL EVALUATION OF THE RF-101 FORWARD OBLIQUE WINDOW UNDER STRESS AND EFFECT OF AIR DENSITY CHANGES ON AERIAL PHOTOGRAPHY

M. P. Moyle
P. L. Jackson
E. K. Dabora
P. Sherman
R. E. Cullen

The University of Michigan

April 1957

Engineering Research Institute Project No. 2508-1-F
Aircraft Propulsion Laboratory
Contract No. AF 33(616)-3459
Project No. 6(7-6273)

United States Air Force
Wright Air Development Center
Air Research and Development Command
Wright-Patterson Air Force Base, Ohio

FOREWORD

The work included in this report was conducted under The University of Michigan Engineering Research Institute Project 2508, and was monitored by the Aerial Reconnaissance Laboratory, Directorate of Laboratories, Wright Air Development Center, Wright-Patterson Air Force Base.

TABLE OF CONTENTS

LIST OF ILLUSTRATIONS

ABSTRACT

This report consists of two parts. Part I is an experimental evaluation of the RF-101 forward oblique window under stress. Part II is subdivided into sections: (A), which deals with experimental investigation of the effect of shock waves on resolution power in aerial photography, and (B), which deals with the problem of the deflection of light rays due to variation in fluid density.

In Part I, a pressure chamber was used to obtain rupture stress data on commercial plate glass. Three sizes were tested: 4 x 4 x 1/8 in., 8 x 8 x 1/4 in., and uncoated RF-101 forward oblique windows. The lowest breaking stress value for each of the sizes of glass was between 3092 and 3600 psi. The average breaking stress of the uncoated RF-101 forward oblique windows was 3938 psi.

Only one coated RF-101 forward oblique window was tested. This window broke under thermal stress only. No pressure was applied. The center of the window's inner surface was maintained at 85°F with the outer surface at 21°F. The crack in the window occurred under apparently steady-state temperature conditions.

Of the many possible causes of the breaking of the coated window, the most probable appears to be the stress caused by the relative change in dimension between the cooled mounting plate and the heated window. The everseal tape spacer used between the window and the mounting frame may not be compressible enough to absorb this relative change in dimension without causing undue shear stress on the window. The high coefficient of thermal expansion of the RF-101 honeycomb nylon phenolic nose section could render the problem of relative change in dimensions more critical.

It was intended to vary pressure and temperature on the heated window simultaneously, simulating critical flight conditions. However, this was not possible after the only available window broke under thermal strain only.

In Part II-A, an experimental investigation of the effect of shock waves on the resolution power of a particular optical system is described. The shocks were produced in The University of Michigan blow-down wind tunnel by a wedge of effective half angle of 7° at three different Mach numbers, namely, 2.50, 2.93, and 4.63. The intensity of the shocks was such that collimated rays from USAF target suffered deviations of 1.46, .89, and .18 seconds, respectively. Photographs of the target with light passing through the shock waves showed practically no difference in the resolution power when compared with photographs of the same target in the absence of shock waves.

Since the deviations of rays parallel to the optical axis of the forward camera in the RF-101 can possibly be larger than those attained in the laboratory, no direct conclusion could be made with regards to the resolution power loss in actual flight. It is concluded that further experimental studies are necessary before effects of shock waves on photography in actual flight could adequately be assessed.

In Part II-B, the problems of determining density fields for different flow configurations and suggested areas of research in connection with obtaining optimum quality photographs are discussed.

OBJECTIVE

The object of this report is (1) to evaluate experimentally the effects of the thermal and dynamic load stresses on the RF-101 forward oblique window and (2) to investigate experimentally the effect of shock waves on the resolution power in aerial photography and to discuss the problem of light ray deflection due to fluid density changes.

PART I

EXPERIMENTAL EVALUATION OF THE RF-101 FORWARD OBLIQUE WINDOW UNDER STRESS

INTRODUCTION

Under flight conditions the forward oblique window is subjected to considerable thermal and pressure stress.

For example, at altitudes from 25,000 ft to 50,000 ft above sea level at Mach 0.8 the outside surface temperature of the window is calculated at 18°F to 20°F while the inside surface temperature is maintained at 85°F (Figure 15, Phase Report No. 1, October, 1954). In a 30° Mach 0.8 dive from 25,000 ft to sea level the outside surface temperature has been shown to rise from 20°F to 115°F within 35 seconds, and to rise to a maximum of 165°F at continued sea level flight. The pressure difference between the inside and outside of the window during the same period will rise from approximately 1 psi to approximately 7 psi (Figure 15, Phase Report No. 1, October, 1954, and Figure 8, YRF-101A, 11-11-55, McDonell Aircraft Corp.).

The thermal stress is made more severe due to these constantly changing parameters. Under such changing conditions, temperature gradients through the thickness of the window may be extremely steep at some distances from the window surfaces. That is, a relatively fast temperature change is incident upon a material with relatively low thermal conductivity.

In steady-state at 25,000 ft the temperature profile through the window thickness approaches a straight line, as in Curve A, Figure 1. This is a comparatively moderate thermal stress.

Curve B, Figure 1, approximates the temperature profile after a steep climb to 25,000 ft from a low altitude, where the window is taken from a sea level steady-state of 85°F throughout the window thickness to 20°F on the outside surface. If the aircraft remains above 25,000 ft long enough to approach closely a steady-state temperature profile, then dives at Mach 0.8 at an angle of 30° to sea level so that the outside window temperature rises from 20°F to 115°-165°F, the temperature profile across the window thickness will assume the form of Curve C, Figure 1.

Curves B and C of Figure 1 indicate steep temperature gradients across the window thickness. The window is more severely stressed under these transient conditions.

In view of the window's geometry, the mounting and edge effects including mechanical stresses from the frame, thermal stresses due to temperature differences between the window and the frame, stresses due to irregular heating caused by non-uniformities of resistance of the conductive coating, and the simultaneous pressure and thermal stresses under flight conditions, theoretical prediction of a safety factor for the window would be inadequate if not impossible.

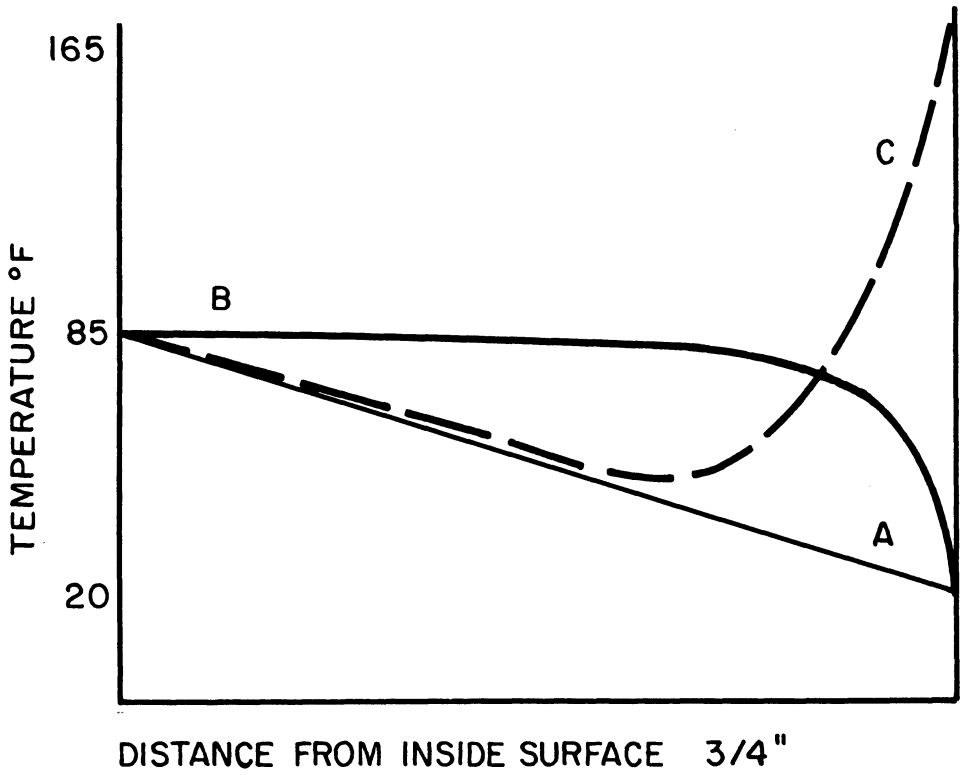

Figure 1. Approximate temperature gradients across forward oblique window thickness.

A. Steady-state at 25,000 ft.
B. After climb from sea level to 25,000 ft.
C. After dive from 25,000 ft to sea level.

Also, experimentally determined breaking-stress data from glass are conventionally obtained by point or line pressure between two supports upon which a strip of glass is resting. Accepting the breaking-stress coefficients so determined to predict thermal and pressure safety factor for an irregularly shaped and semi-fixedly held window is questionable at best.

Experimental simulation of predicted temperature and pressure conditions of actual flight was, therefore, considered necessary to determine a safety factor for the window.

DESCRIPTION OF SYSTEM

For experimental simulation of actual flight conditions, a pressure chamber was constructed with temperature, pressure, and strain instrumentation as shown in the block diagram of Figure 2. Figure 3 is a photograph of the pressure chamber.

The window is mounted on the pressure chamber with thermocouples and strain gages attached to the window surfaces. A pressure transducer is attached to the pressure chamber. These are instrumented to the recording oscillograph.

For temperature variation cold methyl alcohol, tap water, and hot water are introduced into the pressure chamber through three adjustable valves. An outlet is controlled by another adjustable valve.

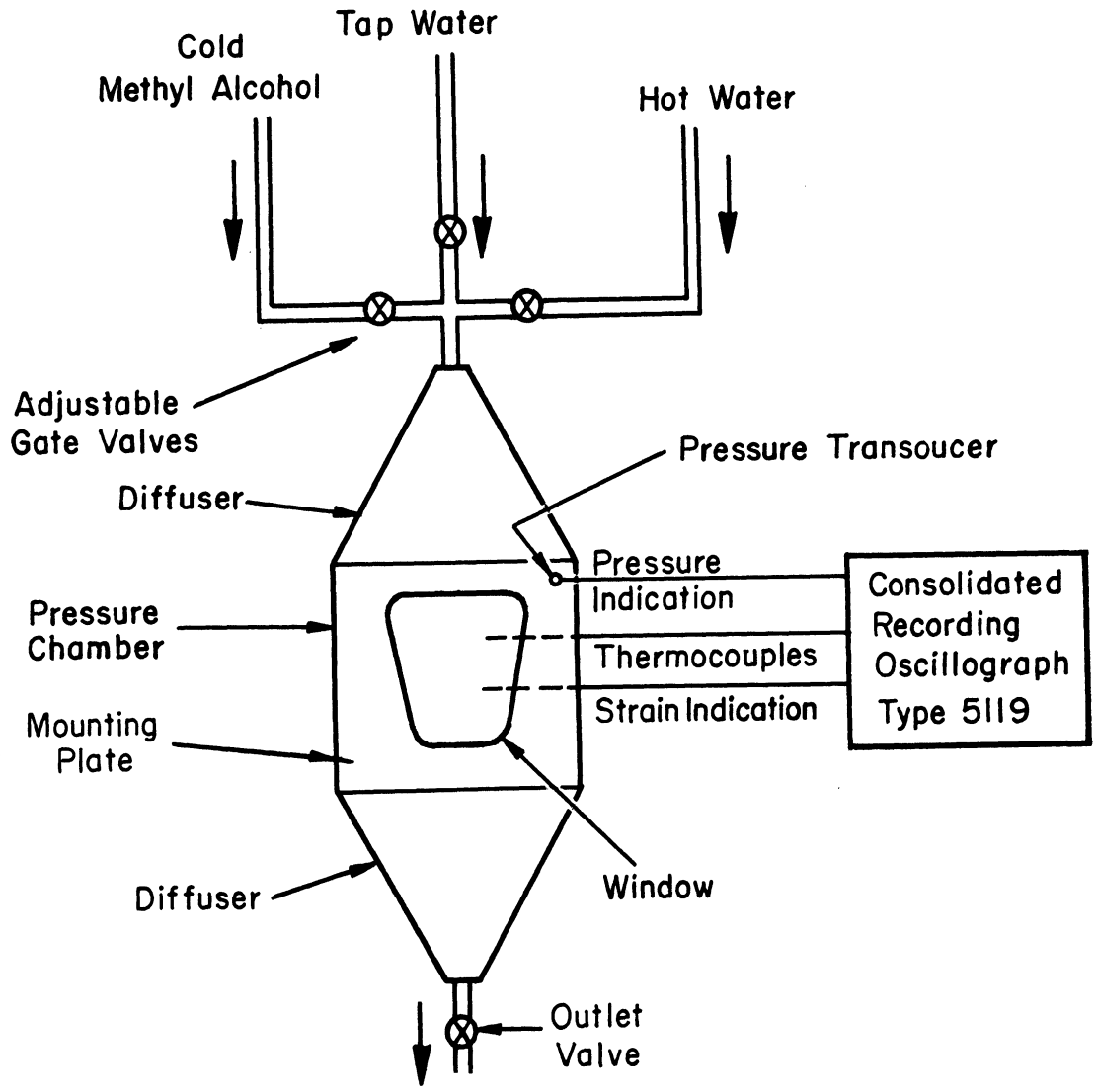

Figure 2. Schematic diagram of experimental setup.

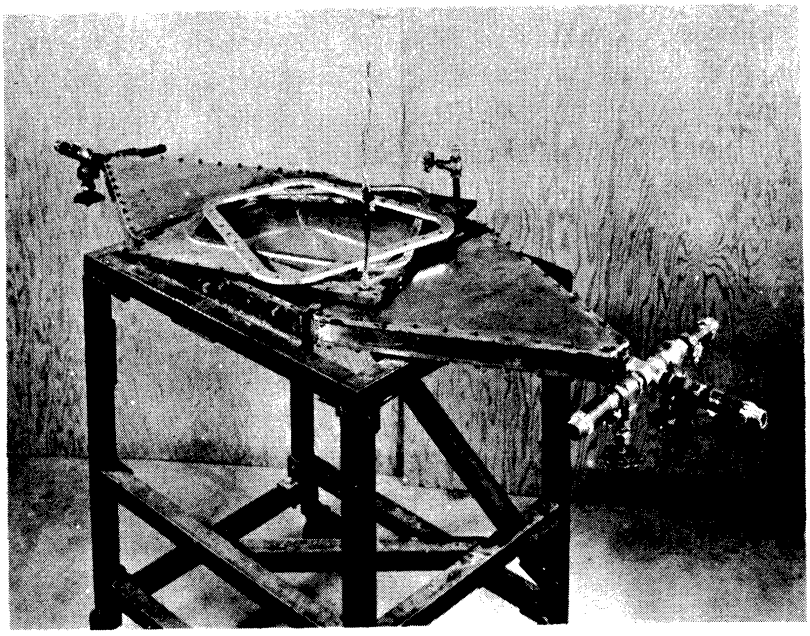

Figure 3. Pressure chamber showing mounting plate, spacer, and retaining ring.

With proper adjustments of the inlet and outlet valves, pressure chamber temperature and pressure profiles are created and recorded, simulating flight conditions on the window. The temperature of the outside window surface is controlled by the temperature and velocity of the fluid passing over the window, while the pressure is adjusted by the relative openings of the inlet valves with respect to the outlet valve.

EXPERIMENTS

PHASE 1

Fifty-six commercial plate glass specimens 4 x 4 x 1/8 in. with square sides and ground corners were destructively tested while mounted on the pressure chamber. Figure 4(a) illustrates the mounting of these specimens. The specimens were subjected to pressure by introducing tap water into the pressure chamber at a rate of approximately 1/2 psi per second until the glass ruptured. No attempt was made to control temperature. Environmental temperature was 80°-85°F, and average tap water temperature, 60°F. Rupture values of 56 specimens tested in this manner are shown in the bar graph of Figure 5.

Glass of a different size and shape from that of the forward oblique window was used for the following reasons:

The glass was readily available and of low cost, so that a comparatively large number of samples could be tested.

The stress placed on the small glass samples is the same type of stress (pressure loading) as that on the forward oblique window when in flight, whereas other obtainable stress data have been obtained by line or point pressure on a glass bar, as previously described.

The need to develop skill in mounting the glass, in operating the pressure chamber, and in using the instrumentation.

It is important to note the following differences when considering the data of Figure 5 with respect to the forward oblique window.

Glass Specimen	Forward Oblique Window
1. Square	1. Trapezoidal
2. Sharp corners	2. Corners rounded to radius of 2 in.
3. Edges perpendicular	3. Edges beveled 30° for 2/3 of thickness
4. No everseal tape spacers used in mounting	4. Six everseal tape spacers between glass and frame
5. Mounting holds from underneath along bottom surface	5. Mounting holds from underneath only along bevel
6. Mounting retainer ring extends 3.1% of the mean distance across the glass plate	6. Mounting retainer ring extends 4% of the mean distance across the glass window
7. Much smaller size	
8. Commercial plate glass	8. Pittsburgh crown glass

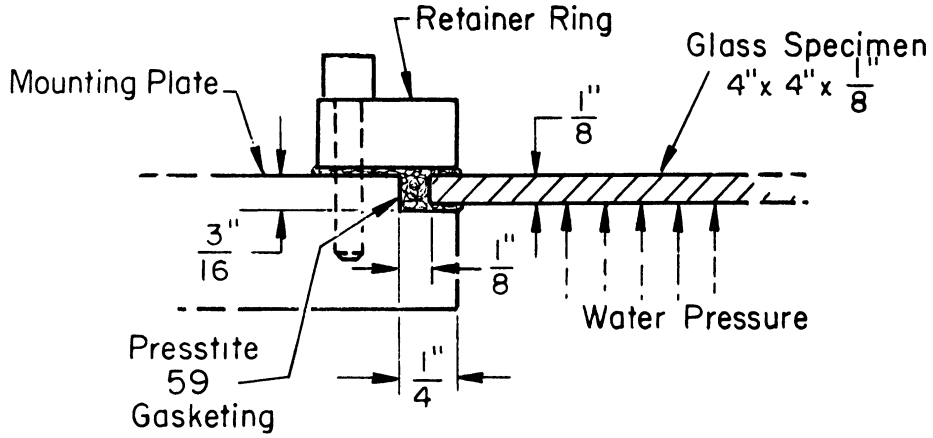

Figure 4(a). Cutaway view of mounting of 4" x 4" x 1/8" glass specimens.

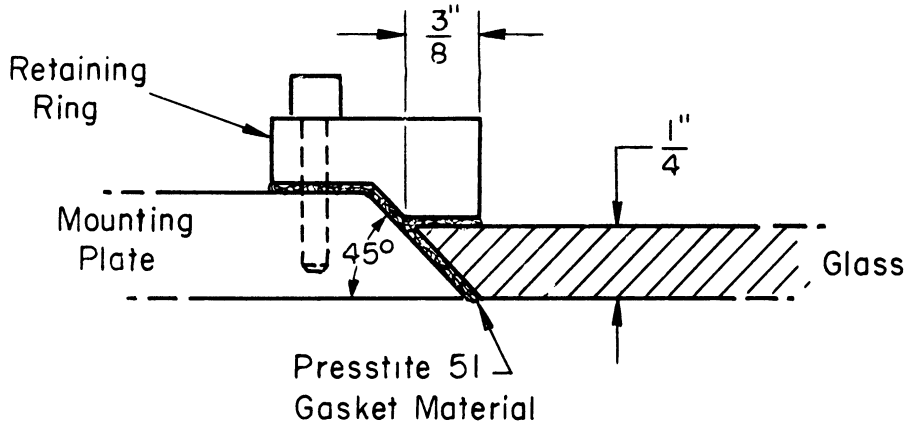

Figure 4(b). Cutaway view of mounting of 8" x 8" x 1/4" glass specimens.

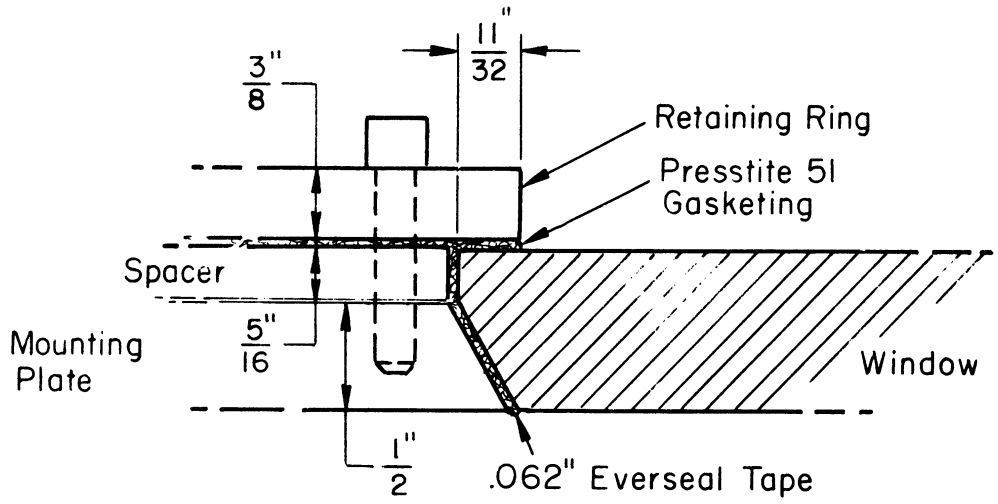

Figure 4(c). Cutaway view of photographic window mounting at spacer.

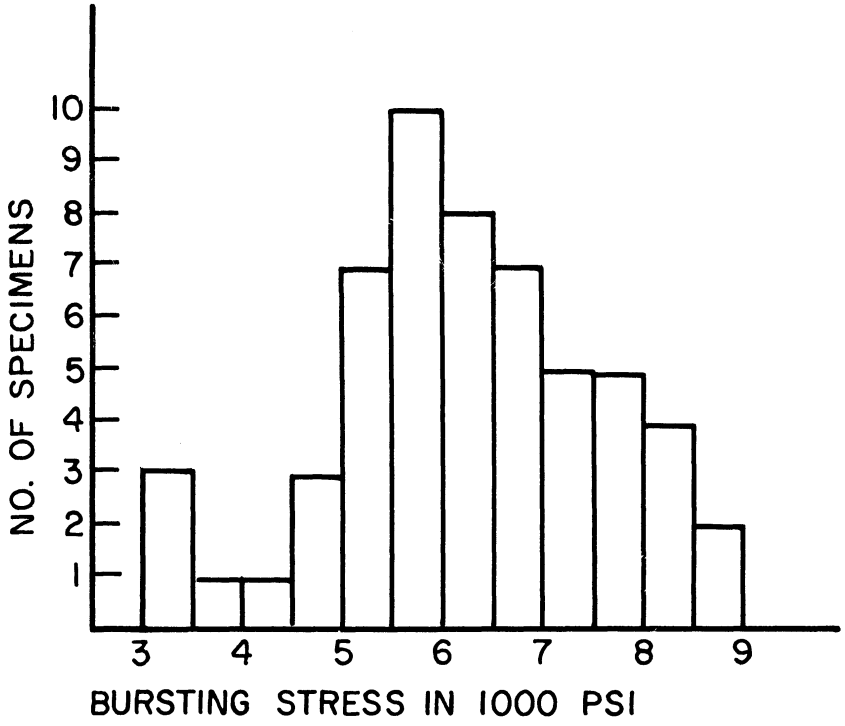

Figure 5. Bursting stress values of 4" x 4" x 1/8" glass specimens.

PHASE 2

Glass plates 8 x 8 x 1/4 in. with 45° beveled edges were destructively tested under conditions identical with those of Phase 1. With the exception of nos. 3 and 5, all the distinctions noted above for the 4 x 4 x 1/8 in. size apply to the 8 x 8 x 1/4 in. size. Figure 4(b) illustrates the mounting. Figure 6 is a bar graph showing the bursting stress values obtained.

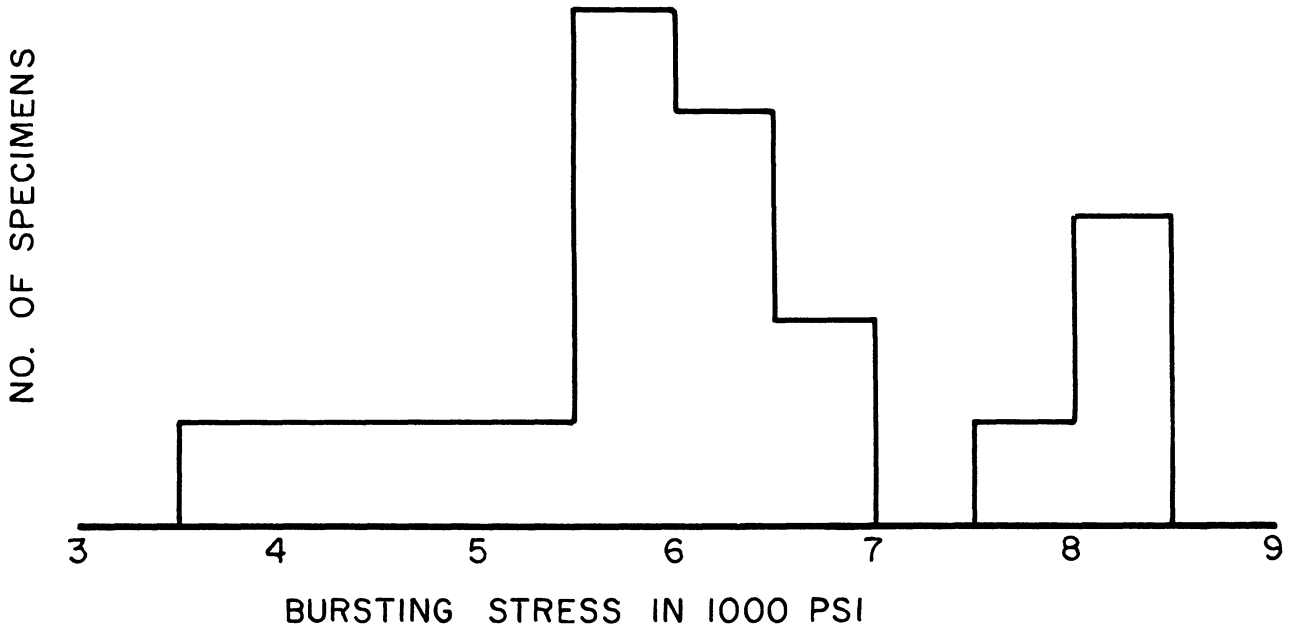

Figure 6. Bursting stress values of 8" x 8" x 1/4" glass specimens.

Six uncoated forward oblique windows, finished identically to the coated window but of commercial plate glass, were furnished The University of Michigan by Liberty Mirror Division of Libbey-Owens-Ford Glass Company.

Breaking pressures of these windows were determined when mounted on a steel plate with an aluminum spacer and retaining ring. All dimensions were identical with the mounting section of the RF-101 nose section. Table I is a tabulation of the breaking values.

TABLE I

BREAKING PRESSURES AND STRESSES OF THE COMMERCIAL PLATE UNCOATED WINDOWS

No.	Psig	Stress
1	45	5374
2	46	5494
3	44	5255
4	33	3941
Avg.	42	5016

Four of the six uncoated windows were subjected to pressure destruction. The method of attaching thermocouples to the glass surface and the adjustment for uniform temperature control of the flow geometry through the pressure chamber was developed using uncoated glass window 6. This window has not been ruptured. It has been withheld for possible mounting on the nose section.

The windows were broken under water pressure, leaving the fissure patterns intact. Pictures of windows 2 and 3 are shown in Figures 7 and 8. Note that the crack patterns fan out from one point on the side. A 64-frame/second moving picture was made of window 4 breaking. The entire fissure pattern appeared between two frames.

Windows 1 and 4 also left fan-shaped patterns emanating from one point. On window 1 this point was at the edge of an everseal tape spacer. In other respects the fissure patterns of all ruptured windows were identical. One effect not apparent from the pictures was the splitting of the glass parallel to its surface. This occurred approximately 1/4 in. below the surface opposite the pressure force, on individual areas of one to six square inches totaling approximately 3% of the area of each window.

The first window was damaged in mounting due to wrong dimensions of the mounting plate.

Window 4 was subjected to twelve slow pressure cycles from 0 to 25-35 psig after it had failed to break at 45 psig, the maximum pressure available for the particular test. This indicates a probable influence of fatigue upon the glass strength. A fatigue effect was noted earlier when commencing the testing of the 4 x 4 x 1/8 in. glass. In developing and testing the instrumentation, individual glass specimens

Figure 7. Uncoated commercial plate glass no. 2 after rupture.

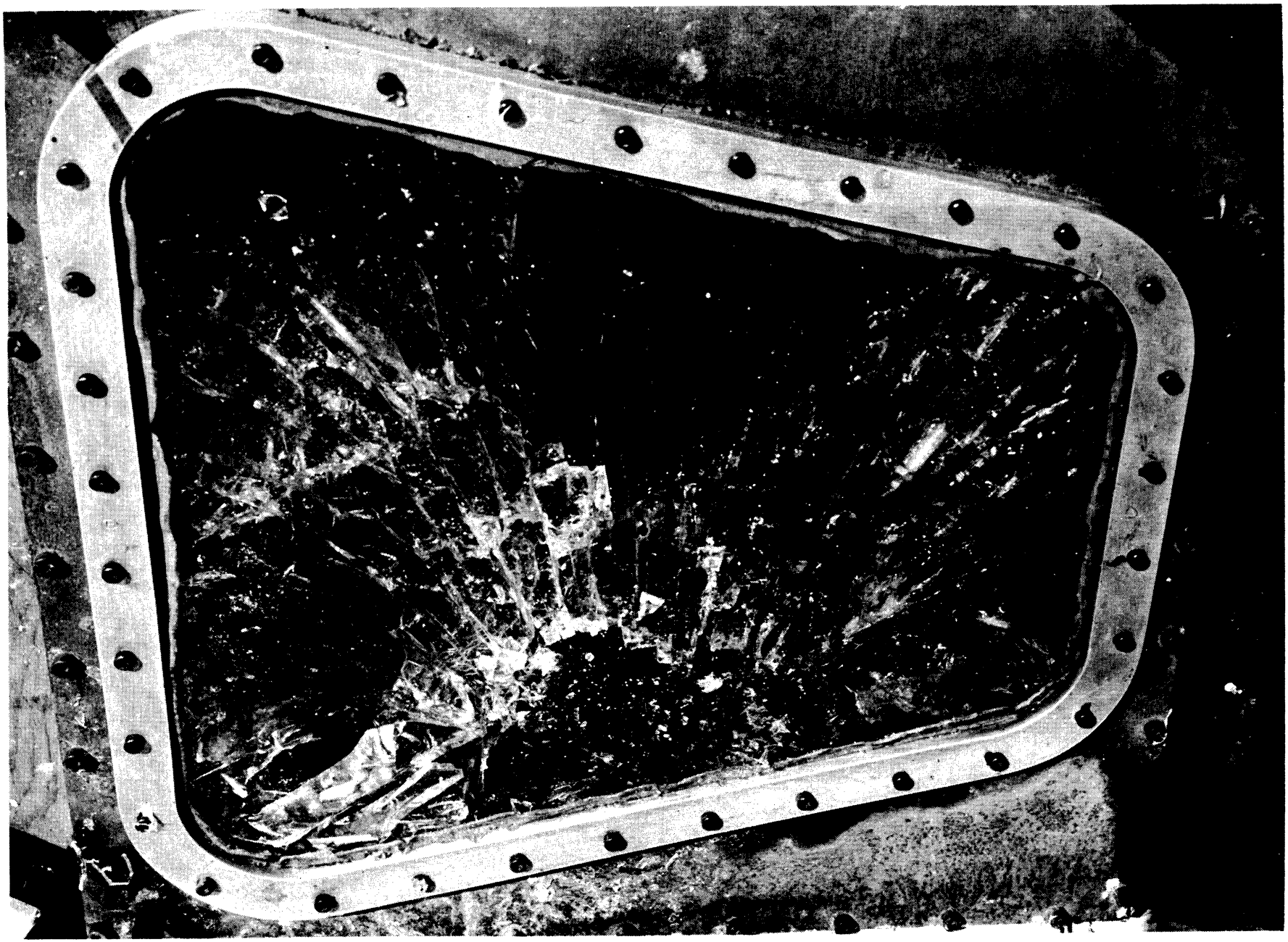

Figure 8. Uncoated commercial plate glass no. 3 after rupture.

were subjected to many pressure cycles. It was observed that some of these specimens ruptured at a lower pressure level than the pressures to which they had previously been exposed. Unfortunately the number and magnitude of cycles and the rupturing pressureswere not recorded, as the primary concern was determining, installing, and calibrating the instrumentation.

PHASE 4

The three previous phases were preliminary to this phase—the testing of coated windows by simulating flight conditions. At least five windows were expected and needed. However, only one was received, and the results of this phase are inconclusive.

Instrumentation.—For the first series of tests, five iron constantan thermocouples were attached to each surface of the window at locations shown in Table II. This distribution was to determine and record the uniformity of temperature in the fluid flow across the outside surface, and the uniformity of heating of the conductive surface of the window.

The junction of an acetylene flame-fused thermocouple was compressed between tool steel rollers to .005-in. thickness, and the flattened part trimmed to a circle of 3/32-in. diameter. As the coated surface of the window is a conductor with a potential across it, a direct connection between the surface and the thermocouple might induce external emf in the thermocouple. An insulation with high electrical resistance and low thermal resistance was therefore needed between the thermocouple junction and the window surface. Mylar tape of .002-in. thickness was found suitable for this purpose.

Before mounting, the thermocouple junction was heated and pressed against the surface of a 3/16 x 1/8 x 1/64 in. celluloid mat until the thermocouple's contacting face was in the plane of the celluloid surface. With the Mylar tape on the thermocouple face, the celluloid mat was cemented to the window surface.

For the following series of tests, only pressure and temperature were to be measured, with a series of strain measurements contemplated for later.

Testing Procedure for Forward Oblique Window.—

Step 1. Bench test. Check for flaws. Place potential across unmounted window. Record temperature versus time at 5 points on face of window.

Step 2. Mount window on pressure chamber in accordance with McDonnell Specification No. 249105.

Step 3. Pressure check to 25 psig by introducing tap water in the chamber, no potential on window.

Step 4. With tap water, cool the outside of window to approximately 43°F. Apply potential across window, increase slowly until steady-state of 85°F is reached on the inner window surface. Measure wattage.

Step 5. Introduce methyl alcohol at 15°F to bring outside surface of window to 20°F. Bring inside of window to 85°F. Measure wattage at steady-state.

Step 6. Temperature profile. With inner window surface at 85°F, raise outer surface from 75°F to 165°F linearly in 30 seconds.

Step 7. Temperature profile. With the outer window surface at 45°F, raise inner surface to 85°F. Raise outer surface temperature linearly to 165°F in 45 seconds.

Step 8. Temperature profile. With outer window surface at 20°F, raise inner surface to 85°F. Raise outer surface temperature linearly to 165°F in 45 seconds.

Step 9. Temperature and pressure profile. Room temperature to 165°F. Increase pressure linearly from 1 to 6.5 psig in 45 seconds; hold at 6.5 psig from 46-60 seconds. Hold outer surface at room temperature from 0-15 seconds; then raise linearly from room temperature to 165°F in period from 16-60 seconds. Inside window surface temperature is held at 85°F.

Step 10. Temperature and pressure profile. Pressure raised from 1 to 6.5 psig in period from 0-45 seconds, held at 6.5 psig from 46-60 seconds. Outer surface temperature at 45°F during period from 0-15 seconds, then raised linearly from 20°F to 165°F during period from 16-60 seconds.

Step 11. Temperature and pressure profile. Pressure linearly raised from 1 to 6.5 psig during period from 0-45 seconds, and held at 6.5 psig from 46-60 seconds. Outer window surface temperature held at 20°F from 0-15 seconds, then raised linearly from 20°F to 165°F during period from 16-60 seconds. Inner surface held at 85°F.

Steps 12, 13, 14. Double maximum pressure (1 to 13 psig), during same time that pressure increased from 1 to 6.5 psig in former steps. Use corresponding temperature profiles of steps 9, 10, 11.

Step 15 and higher. Increase the maximum pressure in increments of 5 psig, using the previous temperature profile from 20°F to 165°F for each step.

Continue in this manner until window is ruptured.

This series of tests is designed to place increasingly severe stress on the window until rupture occurs. In this way the calculated severe flight temperature and pressure conditions are exceeded, and a safety factor may be determined.

Results of Phase 4.—

Step 1. Bench test. Heating test for plated window no. 54B 20-76477-19. Leads attached to bus bars by pressure on brass strips. Powerstat transformer used for power adjusts 115-volt a-c line voltage. Alnor type 2300 surface temperature pyrometer used to detect surface temperature. The window is laid uncoated side down. Ambient temperature is 78°F with normal room circulation.

This test indicates nonuniformity of surface heating. The wide end of the window as seen in Table II is cooler than the narrow end, and the right side (on-looking), cooler than the left. If the coating is uniform, the narrower section

TABLE II

BENCH TEST TEMPERATURE MEASUREMENTS ON COATED WINDOW

Location of temperature measurement points:

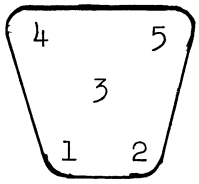

81-E Coated Glass
1, 2, 4, 5 are in corners, 3/4 in. from edges of coating

Time (min)	Powerstat Reading (volts)	Temperature (°F) 1	2	3	4	5
0	20	78	78	78	78	78
10	20	81	81	79	79	79
22	28.1					
40	28.1	94.3	91.5	94	88	84
45	41.0					
62	41.0	112	107	111	98	92

Temperature rise at each point

T_1	112-78	=	34°F
T_2	107-78	=	29°F
T_3	111-78	=	33°F
T_4	98-78	=	20°F
T_5	92-78	=	14°F

Average differences in temperature rises

Top to bottom	14.5°F	1.85 ratio
Side to side	5.5°F	1.26 ratio
Center to top	16 °F	1.94 ratio
Center to bottom	1.5°F	1.05 ratio
Center to left side	6 °F	1.22 ratio
Center to right side	11.5°F	1.53 ratio

Maximum difference in temperature rises between points measured at highest temperature: 20°F 2.43 ratio

would normally heat more than the wider, as the same voltage is applied across each. As $p = V^2/R$, the power p at any particular point or area, and therefore the effective heating of the surface, is inversely proportional to the resistance. Given uniform coating, the resistance is directly proportional to the width of the window.

As noted, the ratio of the temperature rise at the bottom to the temperature rise at the top of the window is 1.85 as measured for an average window surface temperature rise of 26°F. Given a uniform coating, and taking the values of 15-in. width of coating at top, 8.5-in. width of coating at bottom, the difference in power applied may be computed:

$$p \text{ bottom} / p \text{ top} = V^2/R_b / V^2/R_t = R_t/R_b = 15/8.5 = 1.76 \ .$$

Hence, given a uniform surface, the heating of the narrow end would be 1.75 times greater than the heating of the wide end. This is within 6% of the temperature rise ratio of 1.85 found in this test.

It is also noted that the right side averages 5°F cooler than the left side. Visually, it was observed that within three inches of the right side a deeper blue-violet color is reflected from fluorescent light than that reflected from the rest of the surface. This indicates a difference in thickness of the coating on the right side. With a thinner film resistance the power, V^2/R, is lower, and the heating is therefore lessened.

This window, then, was not coated in such a way as to produce uniform heating across its surface.

Step 2. The window was mounted in accordance with McDonnell specifications 249105.

Step 3. The unheated window withstood 25 psig pressure without rupturing.

Step 4. Wattage necessary to maintain inside surface temperature of 85°F while outside temperature is 41°F was determined.

In measuring the voltage across the window, a vacuum tube voltmeter was employed. Inadvertently, the polarity of the voltmeter probes was reversed, so that the ground voltmeter probe was placed on the silver bus bar with the potential above ground. This caused a short circuit, the points of greatest heat occurring on the bus bar at the probe and at the connection to the source. Two darkened, discolored areas 3/16 in. in diameter appeared at these spots. No decrease in conductivity could be detected by an ohmmeter. However, the discolored areas were painted with silver conducting paint.

Under steady-state conditions the following temperatures and voltage were recorded:

Coolant temperature: 41°F
Outside surface: 45°F
Inside surface temperatures: ⟶
Volts: 62.5
Ohms: 26.9
Watts: 145.2

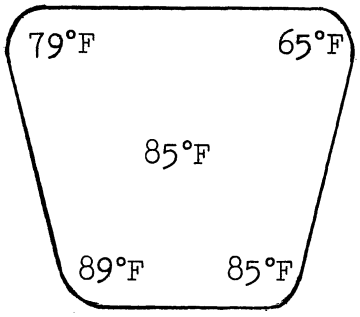

Step 5. Determine wattage necessary to maintain inside surface temperature at 85°F while outside surface temperature is 20°F.

In 18 minutes, the inside surface temperature was raised to 85°F at the center of the glass. At this point the glass cracked under the following conditions:

Coolant temperature: 16°F
Average surface of outside window: 21°F
Profile of surface temperatures: ⟶
Volts: 73
Ohms: 26.9
Watts: 198.1

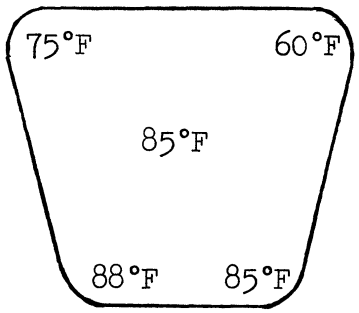

Figure 9 is a photograph of the window after breaking. In testing, the inside window surface is placed downward so the coolant may flow over the outside window surface without air pockets. Methyl alcohol seeping through the crack in the window caused the stained areas.

The photograph of Figure 10 shows the break in more detail. At the leading edge, the crack is 1/8 in. from the everseal tape spacer. On the side the crack is 1/4 in. from the everseal tape spacer, and 1/2 in. from the burnt spot caused by the voltmeter short.

Possible causes for the window breaking include:

1. The thermal stress across the two sides of the glass may have been too great for the window's strength. As previously discussed, with a linear gradient the thermal stress is minimum. The stress is proportional to the temperature versus distance slope. Care was taken in heating the glass surface slowly. However, no data on the temperature gradient at points through the glass were taken, or could be taken without surface destruction. If, then, a sharp gradient slope occurred during testing, a severe strain could have been placed on the window. The indication is that a sharp slope did not occur. Then, assuming the rupture occurred from thermal stress within the window, it is emphasized, from the standpoint of safety, that the window most probably ruptured under the minimum stress condition—a linear gradient.

2. The window might have been pre-stressed, or contained defects which severely weakened it. This is mentioned as a possibility, as it is always a possibility with glass. No such defect was observable, however.

3. The shorting accident with the voltmeter may have weakened the glass by producing "hot" spots. The nearest the crack came to one of the burnt spots was 1/2 in. Considering the duration of the short circuit, the effect of heat would have been much more severe at the spot itself than at a distance of 1/2 in., making this unlikely as the cause of rupture.

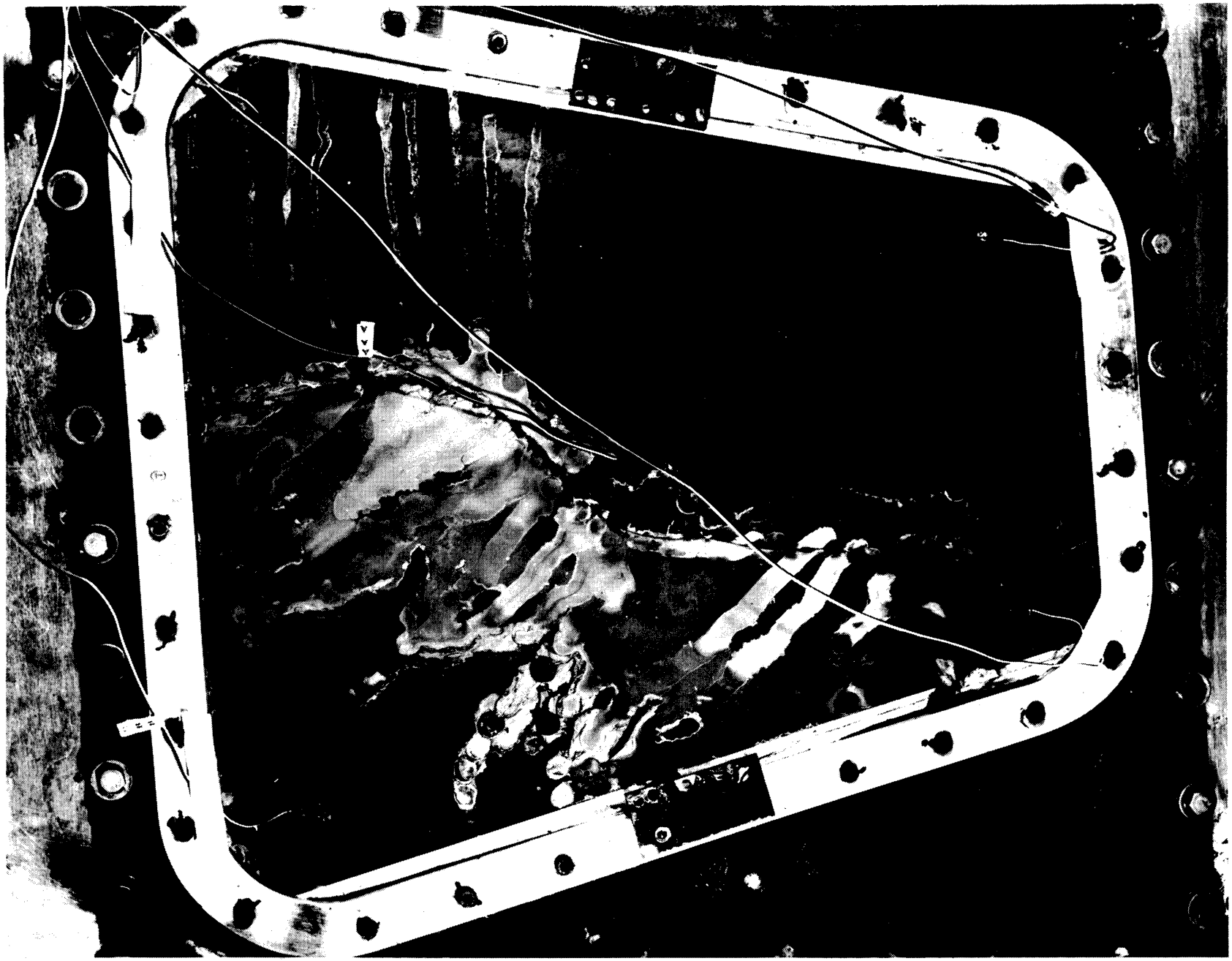

Figure 9. Coated crown glass window (Pittsburgh Plate Glass Co.) after thermal stress rupture.

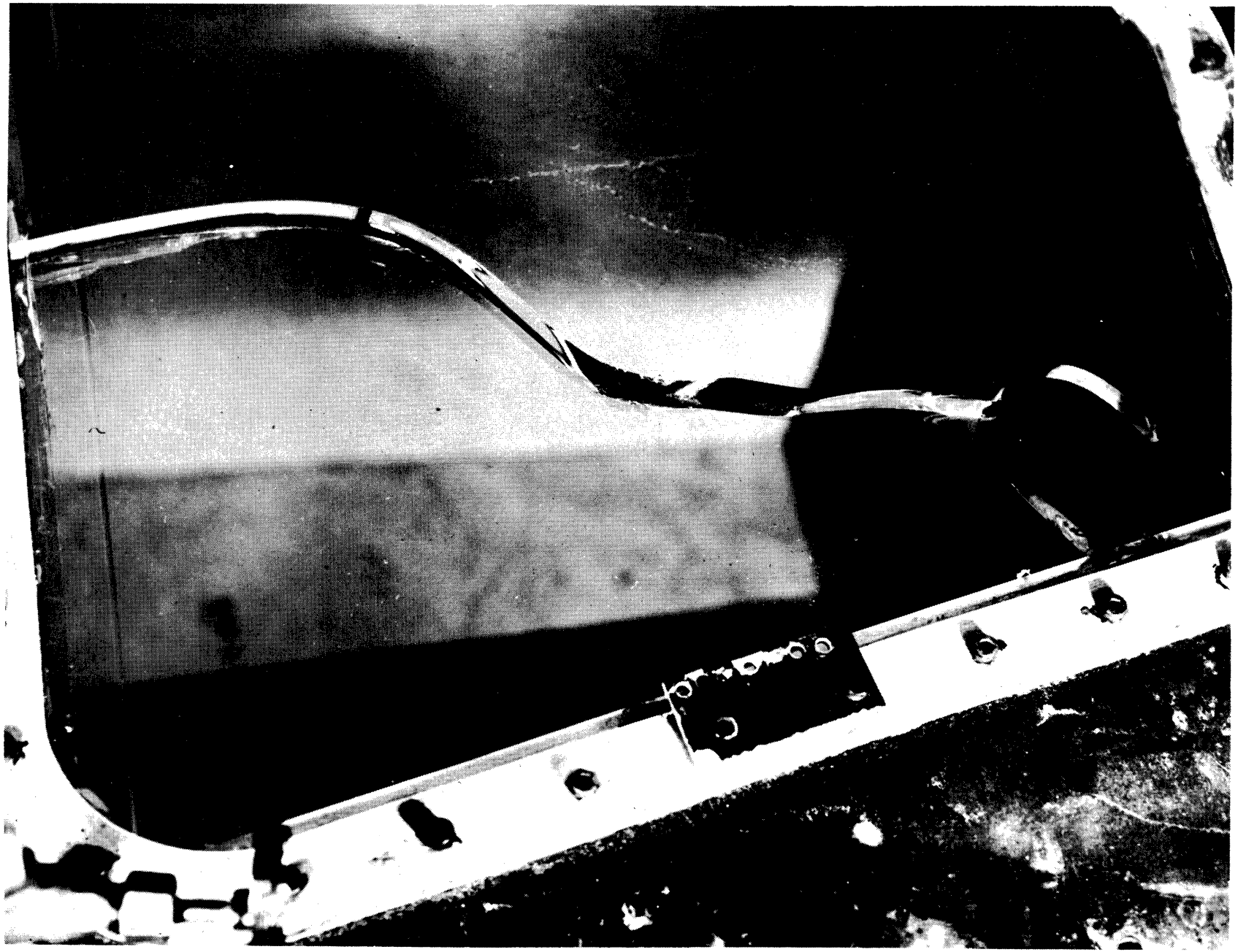

Figure 10. Coated crown glass window (Pittsburgh Plate Glass Co.) after thermal stress rupture—detail of crack pattern.

4. Mounting the glass in the frame may have put a stress on the glass. Presstite 590 sealer and the .062-in. everseal tape spacers were used as gasketing. In disassembly after the window was broken, no contact point between the frame and the window was found, and all the spacer tapes were in place. Pressure applied by the retaining ring through the everseal tape may have contributed to the rupture. However, the window withstood 25-psig pressure. This indicates that undue mounting stress was unlikely.

5. Thermal contraction of the frame. Considering the coefficient of expansion of the steel frame to be $\Delta L/L = 7.2 \times 10^{-6}/°F$, the contraction per 12-in. length would be 5.4×10^{-3} in. As the pressure chamber was covered with insulation and was holding the cold bath, the entire metal holding plate was approximately 21°F. With the inside window surface at 85°F, and with 73°F the ambient when installed, the mounting plate contracted lengthwise 6.1×10^{-3} in. for a 52°F temperature change while the inner window surface expanded 0.98×10^{-3} in. for a relative change in length of 7.1×10^{-3} in. As the window was firmly clamped against the everseal spacer, a direct relative expansion between the window and the frame of .007 in. could exert considerable stress through the 1-1/2-in. spacer. In view of the crack occurring 1/8 in. from the edge of the top spacer, this is a probable cause of rupture.

In actual flight the RF-101 nose section at present is heated only by convective air from the inside, in contrast to the electrical resistance heating of the window.

The nose section is constructed of a core of 6 lb/ft^3 nylon phenolic Honeycomb, 1/4-in. cell structure per mil-c-8073A class 1, type B, with a .020-in. outer skin and a .030-in. inner skin of fiberglas laminate. Commercially available nylon for uses of this type has a minimum coefficient of thermal expansion of $\Delta L/L = 99 \times 10^{-6}/°F$. Ignoring the thin fiberglas laminate skins, the relative change in dimension between the nose section opening and the window would then be 47.4×10^{-3} in. under the thermal conditions of this test.

The original thickness of the everseal tape used for spacers is .064 in. After the spacer was removed from the leading edge its thickness was .032 in. The compressed area is 1-1/2 x 1/2 in. To estimate the stress on the window at this point a preliminary test on compression of everseal tape in an arbor press was made. Approximately 3200 psi were needed to compress the tape permanently to .032 in. However, the time allowed for setting under compression was short.

If a maximum change in relative dimensions of .048 in. occurs, each end spacer would have to compress .024 in. If a single layer of spacer tape is used, and mounting has compressed each spacer .010 in., then a thrust of 4266 pounds on the spacers is possible. This would cause considerable shear stress on the window at the spacer's edge. Given, of course, more compression in mounting, the thrust against the spacer would be greater than 4266 pounds. Even without heating the window, the thermal stress problem may still occur, because of the high ratio of 6 to 1 of the nylon coefficient of expansion to that of glass.

Emphatically, these figures on the comparative thermal expansion of the nose and the window and on the compressibility of the everseal tape are presented only as approximations of the most critical possibilities, to point out an aspect of danger which may not have been considered before.

6. Nonuniformity of heating of the coating. A scratch or gross nonuniformity of the conductive coating thickness may cause a hot spot on the surface of the glass, which in turn causes sharp thermal gradients. No apparent defect of this sort was found on the surface.

7. A sharp gradient may occur between the coated and the uncoated portion of the surface at the bus bars, the top, and the bottom. McDonnell Aircraft Corporation has experienced difficulty with the view-finder windows breaking when a fast rate of heat was applied during bench tests. The breaking was tentatively attributed to the gradient between the area under the bus bars and the coated area when the voltage was applied too quickly. It was felt that either edge heating was needed, or controlled incremental heating.

However, in our experiment the voltage was increased slowly, and the window broke when apparently under steady-state conditions.

CONCLUSIONS

Clearly the experimental work is inconclusive. No performance predictions with respect to the window can be made. Only one coated window was tested, which ruptured under thermal stress. Seventeen experimental steps were contemplated and five completed on one coated window. The precise reason for the window breaking is not known. The breaking may have been caused by:

Thermal stress due only to the temperature gradient through the glass.
Pre-stress or glass defects which were not apparent before mounting.
Experimental procedures—such as possible severe stress on the window by the retaining ring, and an electrical short circuit accident.
Nonuniformity of surface heating.
The thermal gradients between the coated and the uncoated surface around the edge of the inner surface.
The simultaneous contraction of the cooled mounting plate and expansion of the heated window.

The last reason appears the most probable. The relative changes in dimensions due to temperature differences between the mounting frame and the window, coupled with the relatively high pressures necessary to compress the everseal tape spacers, may cause considerable shear stress on the window perpendicular to the ends of the spacers. Considerations of the thermal characteristics of the RF-101 nose section indicate the possibility of a severe shear stress under steady-state conditions at 25,000-50,000 ft.

Results of preliminary experiments with small square plates of glass, and uncoated windows of commercial plate glass ruptured under pressure are included. The uncoated windows ruptured at values between 33 and 46 psig with temperature at 70°F. Some indication of a fatigue factor was found.

Determining a safety factor for the forward oblique window requires tests on many windows under critical temperature and pressure conditions. The result of Phase 4, where the window broke under thermal stress conditions, makes adequate testing more urgent. The experience with the single window pointed up weaknesses in the experimental procedure, and also a possible source of stress in the ever-seal tape spacers.

In further tests, strain measurements should be taken at all times—during mounting, during heating, and when under pressure at any time. This unfortunately was not done during the foregoing tests. If it had been done, more definite conclusions as to the cause of the breaking of the window could have been drawn. In addition to strain gages, the use of a polariscope would detect strain which may not appear on the surface of the glass. The stress on the window under standard mounting procedure should be compared with the stress when mounted without everseal tape spacers. The possibility of stress due to the spacers definitely needs more investigation.

The fatigue effects on the window need investigation. An inverse proportionality exists between duration of the applied stress and the average breaking strength of glass. For example, according to Morey,* investigators have found that glass can support for 0.01 second three times the stress that will break it in 24 hours. Different glass investigators consider the ultimate breaking stress to be from zero to one-half the momentary breaking stress.

It is considered that the length of each successive stress on glass is additive in its weakening effect. Therefore, the effect of successive pressure cycles and the length of time pressures may be applied on the window needs to be determined.

Further tests following the procedure outlined in the report are needed. However, the window should be mounted in the nose section for the experimental tests. This would more nearly duplicate the thermal stress characteristics to be found in flight. It is practical to mount the present pressure chamber on the nose section.

No recommendations, or even indications, of the performance of the window under flight conditions can be made. Extreme caution in the window's use appears advisable.

*George W. Morey. The Properties of Glass. New York: Reinhold Publishing Corp., 1954, pp. 345-6.

PART II

A. AN EXPERIMENTAL INVESTIGATION OF THE EFFECT OF SHOCK WAVES ON RESOLUTION POWER IN AERIAL PHOTOGRAPHY

INTRODUCTION

The problem of light ray refraction due to boundary layer and shock waves has been discussed in references (1), (2), and (3).* It was shown in (2) that deviation through a boundary layer, as long as the boundary layer surface can be assumed as a plane surface, is a function of the Mach number of flight and the altitude, and proportional to the tangent of angle of incidence of the light ray at the boundary layer surface.

In (3), the deviation was shown to be a function of free stream temperature to wall temperature ratio and altitude and again proportional to the tangent of angle of incidence.

This part of the report is mainly concerned with deviation of light rays through shock waves and its effect on the resolution power of aerial reconnaissance photography. The theoretical analysis of the deviation through shock waves is similar to that through boundary layers (2). Light rays suffer deviation as they pass through an abrupt change of density created by the shock wave due to the corresponding change of refractive index of air. The calculation of this deviation can easily be made if one considers two-dimensional shocks (3). However, this becomes more complicated when one deals with curved shocks.

In the experimental work described herein, an attempt to measure the resolution power loss by one optical system through a two-dimensional shock wave is made. Because no experimental correlation has so far been made between light ray deviation and loss of resolution power, it was felt that at the present stage a direct measurement of resolution power would be most useful. Comparison of the experimental results with theoretical calculation of light ray deviation should at least give indication for future work.

DEVIATION OF LIGHT IN McDONNEL RF-101

The deviation of light through shock waves for two possible flight cases of the McDonnel RF-101 is calculated. In each case the deflection of rays parallel to the optical axis of the forward camera is calculated. This axis makes an angle $\theta_o = 15°$ with the horizontal when the flight angle of attack is zero.

Figure 11 shows the path of a light ray when it passes through a shock wave.

*Numbers in parentheses refer to references at end of each section.

A deviation δ is suffered by the incident ray as it passes from one side of the wave front to the other.

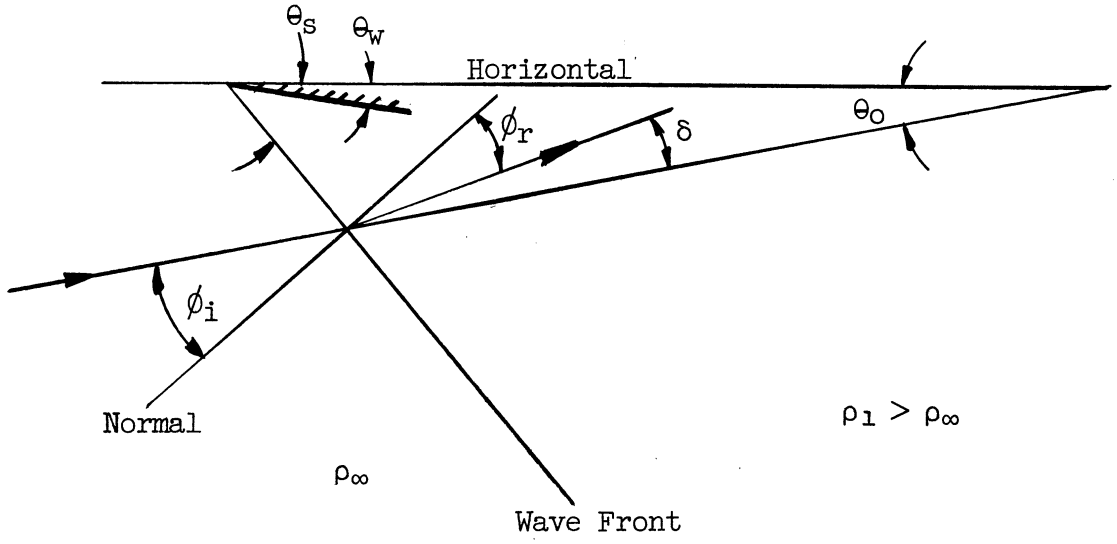

Figure 11. Deviation of light through shock wave.

From (2), one can show that the deviation angle δ can be calculated by the following formula:

$$\delta = \tan \phi_i \frac{k \rho_\infty (1 - \rho_1/\rho_\infty)}{1 + k\rho_1}$$

for small deviations.

If the pitot mast is considered a wedge of 12° and the resulting shock wave, two-dimensional, then at M = 1.5, $\theta_s = 49°$ and $\rho_1/\rho_\infty = 1.238$, and therefore since

$$\rho_\infty = .661 \times 10^{-3} \text{ slug/ft}^3 \text{ at } 35{,}000\text{-ft altitude}$$

$$\delta = -.0184 \times 10^{-3} \tan \phi_i$$

but

$$\phi_i = 90° - \theta_s - \theta_o = 26°$$

for zero angle of attack flight. Therefore, since $k = .117 \text{ ft}^3/\text{slug}$,

$$\delta = -2.84 \text{ sec.}$$

(The minus sign indicates deviation towards the normal.) When the altitude is that of sea level, but the other conditions remain the same, deflection becomes, because of higher density level,

$$\delta = -13.2 \text{ sec.}$$

Thus for the same M the deviation decreases with altitude and for the same altitude the deviation will increase with Mach number.

Unfortunately, in the experimental setup described later, these deviations could not be attained, the prime reason being that only a low density level can be obtained in the wind tunnel used.

Before calculation of the deviation of light in the experimental tests is made, the setup is described.

APPARATUS

The optical system used consists of USAF resolution target, a G.E. flash synchronized with the shutter of a combat still picture, 70-mm camera KE-4 which has 4-in. focal length lens. A 42-in. focal length coated achromatic lens was also provided to collimate the light received from the target. A photograph of the optical system is shown in Figure 12. A sketch of this system showing the relative position of the components with respect to the wind tunnel is shown in Figure 13.

Mountings of the various components were independent of the tunnel and the flash had a separate mount by itself. Thus, it is felt that any vibration in the wind tunnel has little or no influence on the optical system. Furthermore, the flash duration is only 1-2 microseconds, so essentially a vibration-free photograph is taken.

The tunnel is the 4 x 5 in. blow-down University of Michigan Supersonic Wind Tunnel of the variable Mach number type, so runs could easily be made at various Mach numbers. The wedge used to produce a shock has a 5° angle and was mounted by diamond strut at 2° angle of attack, so the effective half wedge angle is 7°. It has a window of approximately 1/4 $in.^2$ in area. In all cases, a 70-mm Super XX film was used.

It was hoped that a 42-in. camera lens could also be used to check the results of the 4-in. focal length lens. This proved to be too sensitive to focal point shift. Also, to get the same exposure, light intensity would have had to be almost 100 times that used for the 4-in. focal length lens if the same flash duration is to be assumed. Such a light source was not available. Long exposure was deemed impractical since vibration effect could be introduced and therefore no conclusive reason could be given to explain any reduction in resolution power.

TEST PROCEDURE

The following procedure was used to conduct the experimental work.

First the optical system was checked for exposure excluding windows in the wind tunnel and the wedge. Then the system was checked again with windows of the tunnel

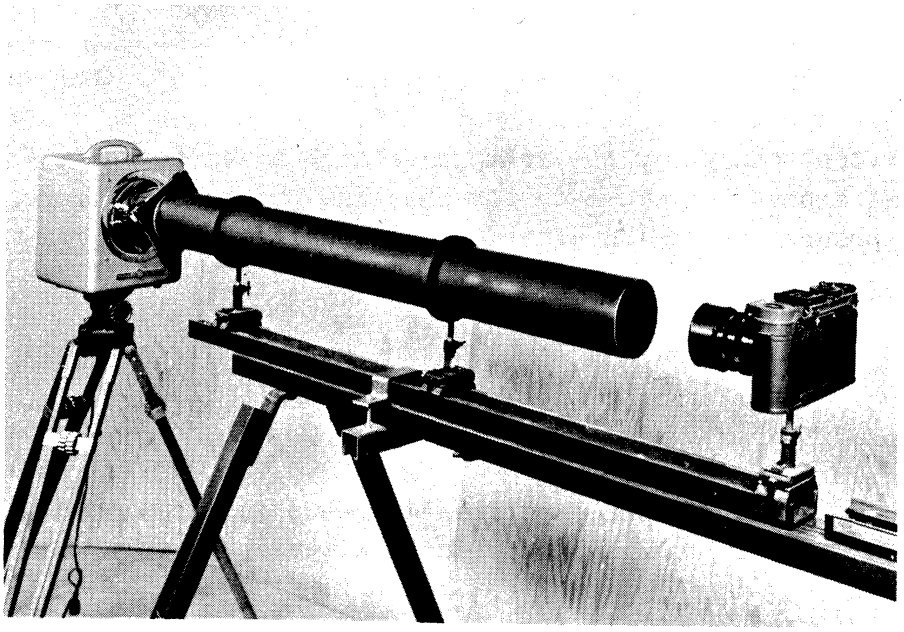

Figure 12. Experimental apparatus, excluding wind tunnel.

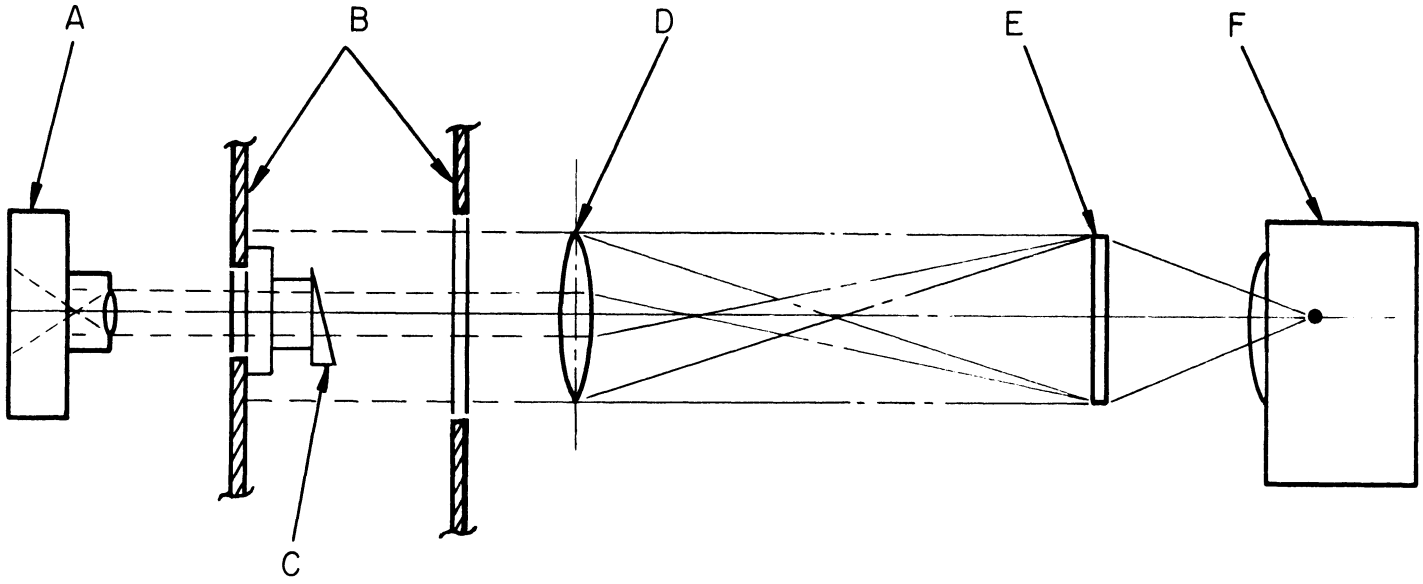

A - Combat camera - KE-4

B - Wind tunnel walls

C - Wedge

D - Collimating lens

E - USAF resolution power target

F - G.E. flash

Figure 13. Schematic diagram of the experimental setup.

and the wedge. No difference was noticed in the resolution power which was about 37 lines/mm. Finally, pictures of the target were taken when flow was introduced at three different Mach numbers, namely, 2.50, 2.93, and 4.63. For each Mach number investigated, pictures were taken under no flow condition to insure that no vibration or inadvertent change in the setup has taken place to shift focusing. In each case, several exposures were made for checking purposes. Figures 15-18 show representative exposures under the experimental conditions.

DEVIATION OF LIGHT IN EXPERIMENTAL SETUP

The deviation of light in the experimental setup is calculated in this section. Figure 14 shows the path of one ray from the USAF target as it passes a shock wave.

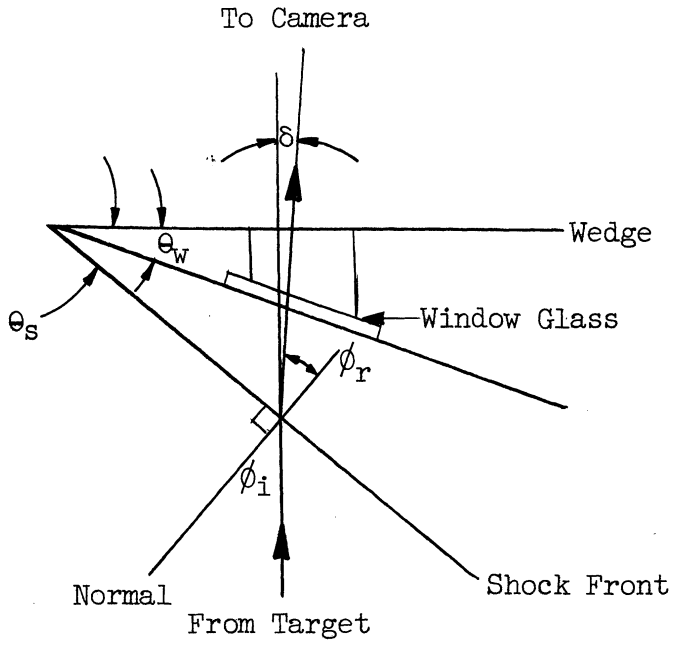

Figure 14. Deviation of light in the experimental setup.

The stagnation density for the wind tunnel is assumed $\rho_o = .232 \times 10^{-2}$ slug/ft^3, and the wedge angle, 7°. From (4) and the equation for δ on page 21 the following table can be obtained:

M	θ_s	ρ_∞/ρ_o	ρ_∞	ρ_1/ρ_∞	ϕ_i	δ
2.50	29°	.1317	$.304 \times 10^{-3}$	1.359	29°	-1.46 sec
2.93	25°	.0822	$.191 \times 10^{-3}$	1.411	25°	-0.89 sec
4.63	17.8°	.0158	$.0365 \times 10^{-3}$	1.707	17.8°	-0.18 sec

It is to be noted here that deviation decreases with increase in Mach number. Also, the conditions for the experimental tests at M = 2.50 is comparable to flight at about 50,000 ft at M = 2.50.

In general, though, these experimental deviations are less than those that could be encountered in actual flight. To simulate flight conditions as far as light deviation is concerned, higher pressure in the wind tunnel would be necessary. The wind tunnel used is being altered to accommodate higher pressures, but unfortunately it will not be completed before expiration date of this contract.

RESULTS AND CONCLUSIONS

1. The experimental tests show no loss of resolution when the variation in the deviation angle was from .18 sec to 1.46 sec. This follows from Figures 15-18, which are photographs of USAF target taken in the absence or presence of shock waves in the light path. As it can be seen, these photographs show practically the same resolution power, with the smallest distinguishable element being 1-5 or 1-6. These photographs are tenfold enlargements of the original negative. Observation of the negatives under a microscope with fivefold enlargement shows the same distinguishable elements. The elements 1-5 and 1-6 correspond to 3.17 to 3.57 multiplied by f_c/f_ℓ, i.e., 33.2 to 37 lines/mm (5).

2. Deviation of light in actual flight can be considerably more than those of the tests. Since no loss of resolution power occurred in the test, it is not very clear what minimum deviation will appreciably affect the resolution power of the optical system used. However, the tolerance on the wedge angle of photographic window glass for the type used in the McDonnell RF-101, namely, Group C (6), is set at 30 sec. If one accepts this as a criterion to give negligible resolution loss, then lower deviations due to shock wave alone in flight conditions considered earlier would have minor effect on the resolution power.

3. Multiplicity of effects should not be ruled out, however. Boundary layers, window glass, curved shocks, the conditions of the atmosphere in the photographic compartment may all have cumulative effects. Only methodical analysis and laboratory tests can lead the way to the understanding of these effects. The technique developed in this paper is believed to be one step in this direction.

RECOMMENDATIONS FOR FUTURE WORK

1. As far as is apparent to the authors, no experimental correlation between deviation and resolution power loss has been made. Such a correlation would seem to be desirable in assessing resolution loss to individual components or phenomena, such as window glass, boundary layer, and shock waves.

2. As aircraft speed is on the increase, higher Mach number tests should be considered to assess both boundary layer effect and shock-wave effect.

3. Since it is more likely that the shocks encountered in flight are curved, tests simulating such shocks should be made. Curved shocks would act almost like a lens with varying curvature and so parallel rays would suffer varying deviations.

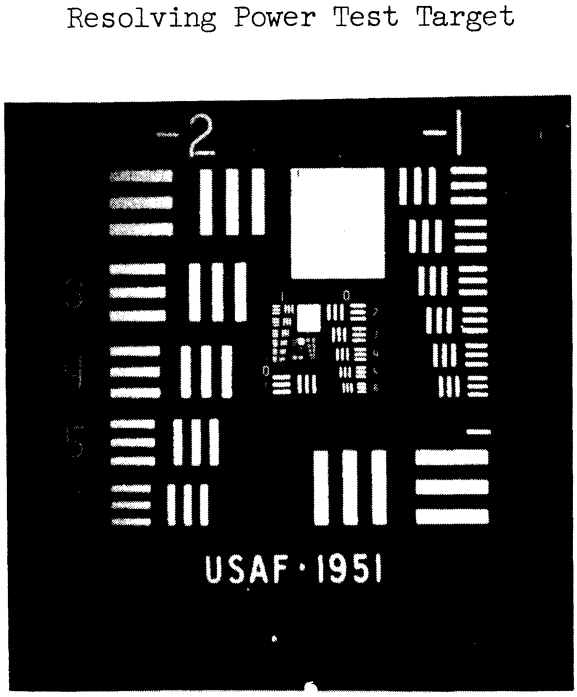

Figure 15. Photograph of USAF target in the absence of shock wave.

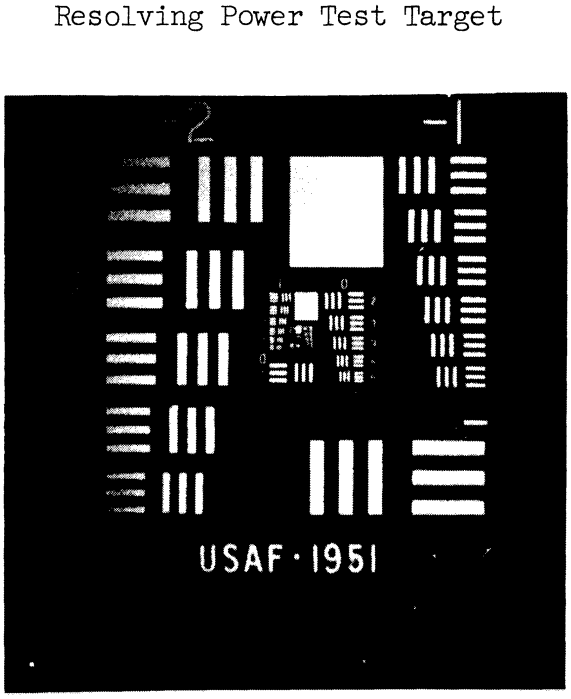

Figure 16. Photograph of USAF target through shock wave at M = 2.50, δ = 1.46 sec.

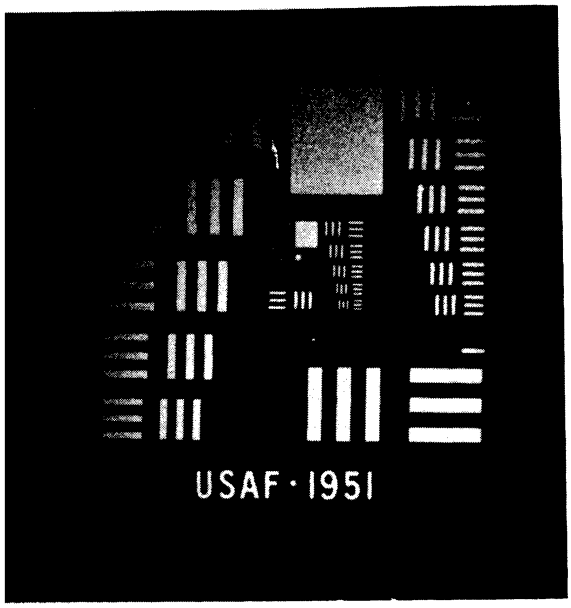

Figure 17. Photograph of USAF target through shock wave at M = 2.93, δ = .89 sec.

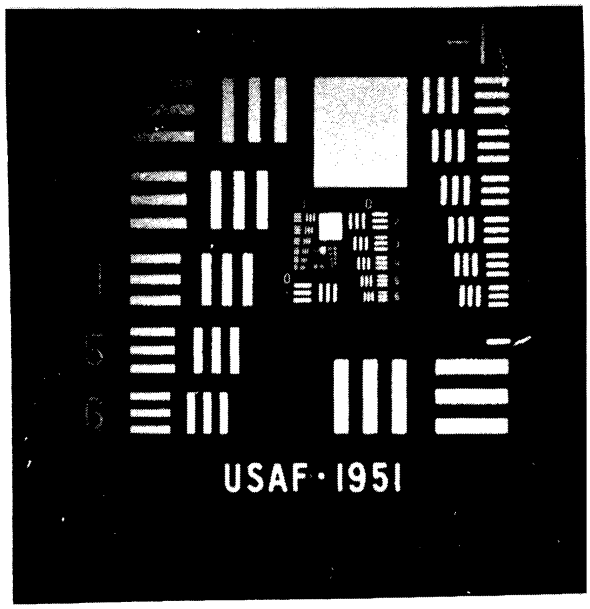

Figure 18. Photograph of USAF target through shock wave at M = 4.63, δ = .18 sec.

The purpose of the tests would be to find the effect of such deviations on the resolution power.

4. Density measurement using interferometer techniques should be made around a model in simulated flight conditions. This will make possible the calculation of deviation.

SYMBOLS

ϕ_i = angle of incidence
ϕ_r = angle of refraction
δ = deviation angle = $\phi_r - \phi_i$
k = air constant in the equation:
($n = 1 + k\rho$) for the refractive index of light where
n = refractive index
= .117 $ft^3/slug$
ρ_∞ = static density in free stream $slug/ft^3$
ρ_1 = static density after shock wave
ρ_o = stagnation density
M = Mach number
θ_w = 1/2 wedge angle
θ_o = angle of optical axis with horizontal
θ_s = 1/2 shock-wave angle
f_c = collimator focal length
f_ℓ = camera lens focal length

1. Moyle, M. P., and Cullen, R. E., "Refraction Errors in Aerial Photography at High Flight Speeds," The University of Michigan, Ann Arbor, Michigan, Engineering Research Institute, Project 2197, January, 1955.

2. Liepman, H. W., "Deflection and Diffusion of a Light Ray Passing Through a Boundary Layer," Douglas Aircraft Company, Report SM 14397, Santa Monica, California, May, 1952.

3. Moyle, M. P., and Cullen, R. E., "Anti-Icing and Anti-Frosting of Aerial Photographic Windows," The University of Michigan, Ann Arbor, Michigan, Engineering Research Institute, Project 2197, October, 1955.

4. "Equations, Tables and Charts for Compressible Flow," NACA Report No. 1135, 1953.

5. Military Specification: "Section 2 Testing and Evaluation of Photographic Lenses," MIL-STD-150, 1950.

6. Military Specification: "Glass, Window, Aerial Photographic," MIL-G-1366B, (USAF), June, 1953.

B. DEGRADATION OF AERIAL PHOTOGRAPHS DUE TO VARIATIONS IN AIR DENSITY

Light rays will be refracted in different amounts by a medium, depending on the density of the medium, the change in density, the wave length of the light, and the angle of incidence of the light ray. The quality of photographs taken from a moving body is, therefore, dependent on the density configuration in the region of the optical path. To optimize the optical system in a supersonic aircraft, for example, one should know for all operating conditions:

the position and form of shock waves;
the density field between the shock wave and the body boundary layer;
the variation of density through the boundary layer; and
the density inside the camera compartment between window and camera lens.

There is a sharp change in gas density at the surface of a shock wave. Light impinging on this surface of discontinuity will therefore be deflected. The angle of deflection is a function of the strength of the shock wave as well as a function of the angle the incident rays makes with the shock surface. If this surface is curved or if there is a spread in the impinging rays, there will be differential refraction. The variation of density further downstream of the shock must also be considered since it further deflects the light rays. Although papers have been written (1,2,3,4) on the position of detached shocks and the flow field behind them, there is still no satisfactory way, as yet, to predict accurately the density field behind a curved shock wave or what its position will be.

Although the change in density in a boundary layer is more gradual than that across a shock wave, large density changes from free stream conditions can exist, so that the boundary layer becomes important in considering the quality of photographs taken through such layers. Approximations have been made (5,6) for simplified boundary layer configurations and some experimental data have been obtained, but the results to date leave much to be desired, both as far as experiment and analysis go. This is particularly true in the region where there is a definite interaction between the viscous boundary layer flow and the "inviscid" outer flow region. That is, where the shock wave is close to the body, the boundary layer growth tends to change the shock-wave shape, and the increased shock-wave strength makes for a decrease in the growth of the boundary layer. Some work has been done (7) on the interaction of shock wave and boundary layer, but as yet a method for reliable prediction of the density field is unavailable and experimental data are limited. Of course, heating or cooling any surface in the optical path (such as the camera window) will change the thermodynamic coordinates in the boundary layer and therefore affect the passage of light through it. Heating or cooling by fluid injection would have an even greater influence.

There is also the problem of turbulence in the boundary layer. A turbulent boundary layer will cause light scattering. This phenomenon has been studied to a very limited extent (5,12) and leaves much to be investigated in connection with aerial photography.

In hypersonic flow where very high temperatures are reached behind shock waves and in the boundary layer, real gas effects must be considered (8,9,10,11). Air can no longer be regarded as an ideal gas. Furthermore, the air may not be in chemical equilibrium. Dissociation, recombination, and ionization, as well as definite variations of such quantities as specific heat and conductivity with temperature, make the prediction of flow fields and the consequent influence on the transmission of light difficult. Values have been computed for thermodynamic quantities of air at high temperatures in the equilibrium state for limited regions. These values have been used in obtaining some fluid dynamic solutions. However, computations for the time or distance to reach equilibrium indicate chemical equilibrium cannot tacitly be assumed.

It should be pointed out that the density inside the camera compartment, that is, between the camera compartment window and camera lens, is of importance inasmuch as a density different from the density outside the window may result in deflection of light coming through the window.

One should note that a poor photographic image may result from the additive effects of the somewhat independent conditions mentioned, each of which by itself may have no noticeable effect. For example, the effect of the boundary layer outside the camera compartment window could add to the effect of a much decreased density between window and camera.

It is clear that there is a need for much analytical as well as experimental investigation of the problems described. Methods for the prediction of density fields in the regions of shock waves and boundary layers should be developed. The direct measurement of the density fields in shock tubes or wind tunnels for simplified configurations, by such means as interferometry or x-ray absorption, would be an important contribution. An analysis of the optical problem resulting from the changing density could then be made and a direct measurement of the change in the photographic image could be obtained as an experimental check, relatively simply. It would seem that in the case of the turbulent boundary layer the most fruitful approach would be to determine gross parameters influencing the passage of light rays. The possibility of obtaining similarity parameters for the optical problems should also be exploited.

In considering simulating conditions for measurement, one should not overlook the importance of the absolute density level of the gas, since refraction is a function of density as well as the change in density. Therefore, if free stream temperature is different from the actual conditions of interest, as it usually is in wind tunnels, both correct Mach number and correct Reynolds number are necessary. Of course, this is correct if one assumes viscosity is proportional to square root of absolute temperature. Otherwise, the same temperature and therefore pressure as in the actual case are necessary for simulation of the optical problem.

Since refraction is dependent on wave length, the fact that most light is made up of several wave lengths should be considered. Chromatic dispersion may be important in the consideration of photographic quality for some conditions.

Of course, in each case, for a given aircraft and set of operative conditions, an analysis should be made to minimize, by means of an optimum optical system-body geometry, effects detrimental to the photographic image obtained. Such considera-

tions as the position of the camera optical axis in relation to the aircraft body surfaces are important in minimizing differential refraction.

REFERENCES

1. Maccoll and Codd, "Theoretical Investigations of the Flow Around Various Bodies in the Sonic Region of Velocities," Theoretical Research Report Number 17/45, Armament Research Department, British M.O.S., September, 1945.

2. Moeckel, W. E., "Approximate Method for Predicting Form and Location of Detached Shock Waves Ahead of Plane or Axially Symmetric Bodies," NACA TN 1921, 1949.

3. Busemann, A., "A Review of Analytic Methods for the Treatment of Flow with Detached Shocks," NACA TN 1858, 1949.

4. Li and Geiger, "Stagnation Point of a Blunt Body in Hypersonic Flow," I.A.S. Preprint No. 629, January, 1956.

5. Liepmann, H. W., "Deflection and Diffusion of a Light Ray Passing Through a Boundary Layer," Report SM-14397, Santa Monica Division, Douglas Aircraft Co., May, 1952.

6. Moyle and Cullen, "Refraction Errors in Aerial Photography at High Flight Speeds," The University of Michigan, Ann Arbor, Michigan, Engineering Research Institute, Project 2197-20-P, May, 1955.

7. Lees and Probstein, "Hypersonic Viscous Flow over a Flat Plate," Princeton University Aeronautical Engineering Laboratory Report No. 195, April, 1952.

8. Romig and Dore, "Solutions of the Compressible Boundary Layer Including the Case of a Dissociated Free Stream," Convair Report ZA-7-012, August, 1954.

9. Moeckel, W. E., "Oblique Shock Relations at Hypersonic Speeds for Air in Chemical Equilibrium," NACA TN 3895, January, 1957.

10. Squire, Hertzburg, and Smith, "Real Gas Effects in a Hypersonic Shock Tunnel," Arnold Engineering Development Center Report No. AEDC TN 55-14.

11. Logan, J. G., Jr., "Relaxation Phenomena in Hypersonic Aerodynamics," I.A.S. Preprint No. 728, January, 1957.

12. Baskins and Hamilton, "Preliminary Wind Tunnel Investigation of the Optical Transmission Characteristics of a Supersonic Turbulent Boundary Layer," Northrup Report No. GM 1.27 (AM-170), April, 1952.